Visualization of Unsteady Behavior of Cavitation in Circular Cylindrical Orifice with Abruptly Expanding Part

Yasuhiro Sugimoto and Keiichi Sato
Kanazawa Institute of Technology
7-1 Oogigaoka, Nonoichi-machi, Ishikawa, Japan
y-sugi@neptune.kanazawa-it.ac.jp, ksato@neptune.kanazawa-it.ac.jp

ABSTRACT

Cavitation problems in plant's piping system have been investigated on the basis of high-speed observation. Cavitation is one of the important factors with potential damage in piping system at nuclear power plant. In a power plant, there is cavitation occurrence to be expected in some local places such as an orifice, a valve and a pressure reducer. We have investigated about unsteady behavior and impact of cavitation in a long orifice with an abruptly expanding pipe. In this study, some detailed cavitation behaviors are observed by varying cavitating condition in the orifice throat and downstream of the orifice. High-speed behaviors of cavitation are observed by means of a high-speed video camera with a laser sheet in order to observe the inside of the circular orifice. Then images are analyzed using a frame difference method. As a result, we observe a series of cavitation developing process with decrease in cavitation number such as I: cavitation inception occurs at the inlet of orifice, II: cavitation develops in the throat of the orifice, III: large-scale cavitation clouds appear downstream of the orifice, IV: liquid jet appears when the pressure downstream of the orifice decrease to about vapor pressure. Cavitation clouds in a circular cylindrical orifice with abruptly expanding part show some unsteadiness even in the steady operating condition. Cavitation clouds also show a large-scale shedding behavior in the transition stage to a liquid jet condition. In addition, we observe that the interface instability of a liquid jet downstream of the orifice depends on the cavitation instability in the orifice throat.

KEYWORDS

Cavitation, Long Orifice, Piping System, Cavitation Instability, Image Processing

1. INTRODUCTION

Cavitation is a high-speed phenomenon and shows an unsteady impulsive behavior. The cavitation unsteady phenomenon was investigated by observation to understand its behavior [1]. Cavitation is an important factor in evaluating the damage potential for the piping systems in nuclear power plants. In a power plant, cavitation can be expected in a few localized places, such as an orifice, a valve, or a pressure reducer. The unsteady behavior of cavitation cloud is observed even in the flow field of a circular cylindrical orifice. Unsteady cloud cavitation can cause large pressure fluctuations or severe impacts in the fluid machinery.

On the other hand, the impact and the vibration caused by cavitation can be used positively. The high impact of cavitation is used to increase the machining ability and shot-less peening of a water jet [2],[3]. Generating cavitation in a nozzle can also enhance atomization [4]. If

the influence of unsteady cavitation in a nozzle propagates to the nozzle, then the jet is disturbed. Measuring the detailed behavior of cavitation is one of the most important problems.

Our research group performed simultaneous observations of cavitation behavior with impulsive pulses, using a high-speed video camera and an impulsive force sensor to determine the mechanism of cavitation impacts [5]-[8]. We found that a separated vortex cavitation, generated in flow field around a bluff body such as a circular cylinder showed high impact characterized by a cavitating flow in the transition cavitation stage. We also performed quantitative estimation of cavitation phenomena such as the speed of cavity collapse through the detailed visualization of behavior related to cavitation erosion [9],[10]. We observed that cavities flowed up to a large vortex cavity with pairing and coalescence motion in the shear layer region, and then they shed downstream as a large-scale cavitation cloud [11],[12]. Detailed visualization showed similar unsteady cavitation behavior in a cylindrical orifice [5],[13-15].

Recently, we used image analysis to perform quantitative estimation of a series of images taken by a high speed video camera [16],[17]. We measured behavior related to the propagation of a pressure wave generated by the collapse of cavitation bubbles, using the surrounding bubbles and image analysis. In this study, we focus on a circular cylindrical orifice inserted in a pipeline, and show some measured examples of impulsive and unsteady cavitation behavior.

2. EXPERIMENTAL APPARATUS AND PROCEDURE

2.1. Experimental Apparatus

A closed type cavitation tunnel was used for the experiment, as shown in Fig. 1. The test section has a circular pipe 80 mm in diameter (D) and a circular cylindrical orifice, as shown in Fig. 2. We used two orifices, one with a diameter (d) of 15 mm and length (L) of 70 mm, and the other 22 mm in diameter and 100 mm long. The test section was made of a transparent acrylic resin, so we can observe the inside. There are two pressure taps at 20 mm upstream and downstream of the orifice for measuring the reference pressure. Dissolved oxygen content in tap water, which plays an important role in cavitation inception, is controlled by maintaining a low pressure in the tunnel and by circulating the water. The dissolved oxygen content β was measured by a dissolved oxygen meter [Horiba, OM14].

Bubble behavior was observed with a high-speed video camera (KODAK EKTAPRO 4540) with a maximum recording rate of 40500 frames per second (fps). Recording rates of 9000, 13500, and 18000 fps were used for observation. We used continuous light, and therefore, the frame exposure time corresponds closely to the reciprocal of the recording rate. We used a metal halide light (Photron, HVC-SL, 150W) and an argon ion laser (SOC, GLG3482, 4W) as light sources for visualizing cavitation. A laser sheet of about 3 mm thickness provided illumination for observing a sectional view of the orifice throat (see Fig. 3).

Cavitation experiments were made under a constant free stream velocity by reducing the static pressure of the tunnel. In this study, a liquid jet in air and a submerged liquid jet experiments were performed in a closed cavitation tunnel. In order to examine a liquid jet in air, the downstream part of the orifice is ventilated to remove the water around the jet under the submerged jet condition. The cavitation number σ and Reynolds number Re are defined as,

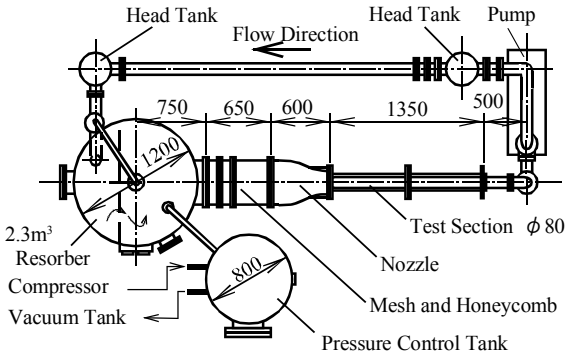

Fig.1 Cavitation tunnel.

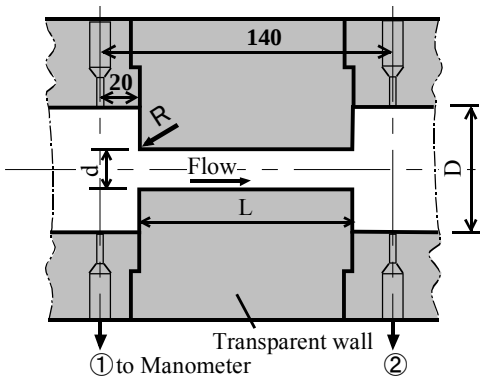

Fig.2 Details of test section.

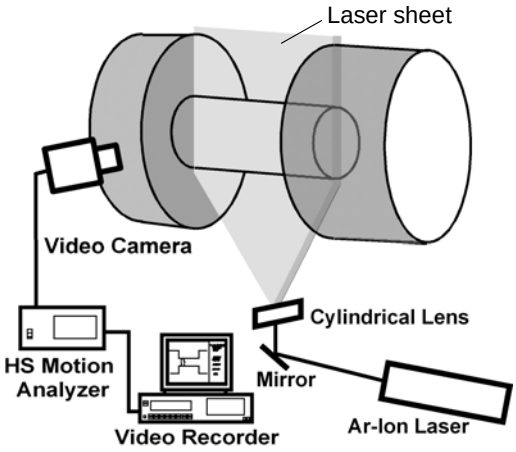

Fig.3 Laser sheet observation system.

$$\sigma = (P_2 - P_v) \ / \ (P_1 - P_2) \quad (1)$$

$$Re_d = Ut \cdot d / v \quad (2)$$

where P_1 and P_2 are static pressures upstream and downstream of the orifice, respectively; P_v is the saturated vapor pressure, ν is the kinetic viscosity of water, and Ut is the mean velocity in the orifice throat ($Ut = 4Q/\pi d^2$, Q is the flow rate of water). In addition, Fs is the recording rate of the video camera.

2.2. Image Analysis Method

The video images taken by the high-speed video camera provide only instantaneous visual information. These images can intuitively show the high-speed phenomenon by viewing them as a movie, however, the movie is unsuitable for quantitatively estimating the motion. We attempted to quantitatively analyze the high speed phenomena related to cavitation by analyzing the pictures using the frame difference method [16],[17]. The frame difference can estimate cavity generation, growth, translation, and collapse by estimating the variations among high-speed images through the difference between two images at different times. In addition, the behavior of pressure waves due to cavity collapse can be estimated by analyzing the deformation and collapse behavior of the surrounding small bubbles.

3. EXPERIMENTAL RESULT AND DISCUSSION

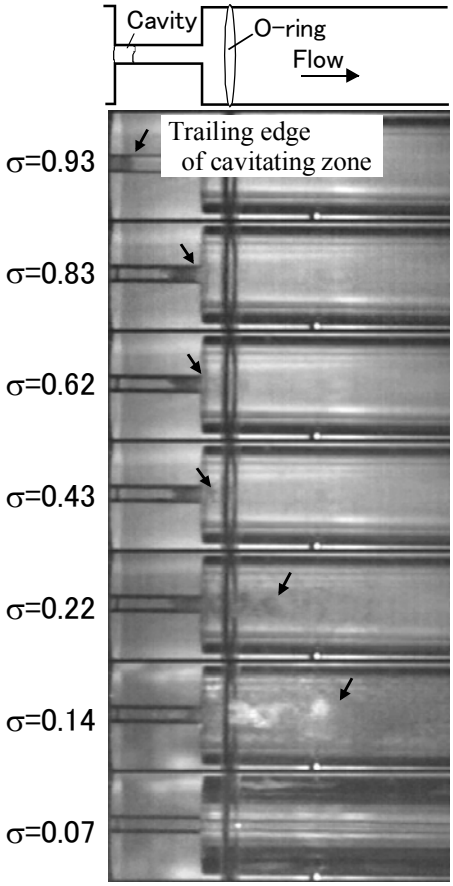

L=70, d=15, R=0: $Re_d=1.3\times10^5$
β = 1.8 mg/ℓ, Q=0.09-0.10m³/s

Fig.4 Liquid jet in water.

3.1. Cavitation Behavior in the Orifice Throat and Submerged Jet

Figure 4 shows the observation result of a cavitating zone at different pressures, under a constant flow velocity. The orifice is 15 mm in diameter and 70 mm long without inlet roundness. Black arrows in the figure indicate the trailing edge of the cavitating zone. With a decrease in cavitation number, the cavitation state changes from inception to the sub-cavitation state, transition-cavitation state, and super-cavitation state in the orifice throat [5]. Under relative high pressure at the orifice exit (σ= 0.93), the cavitating region is limited to the inlet of the orifice throat and there is no cavitation around the orifice exit. Under this condition, the cavitation state transits to the transition-cavitation stage where the cavitation length increases rapidly with a decrease in pressure. In the transition-cavitation stage, cavitation appears that sheds periodically with the periodicity depending on the cavity length, and it becomes less clear as the cavity becomes longer [14].

The cavitation state changes to a super cavitation state by decreasing the cavitation number to about σ= 0.83. The liquid jet detaches from the orifice wall at the inlet of the orifice. Then, the jet re-attaches around the orifice exit where irregular vibration and shedding behavior of the cavity are observed. In this stage, shed cavities collapse in the orifice throat and do not flow downstream from the orifice.

For σ= 0.43, only small-scale cavities shed downstream of the orifice; whereas for σ= 0.22, the flow re-attaches in the orifice as the cavitating region expands to the orifice exit. In case

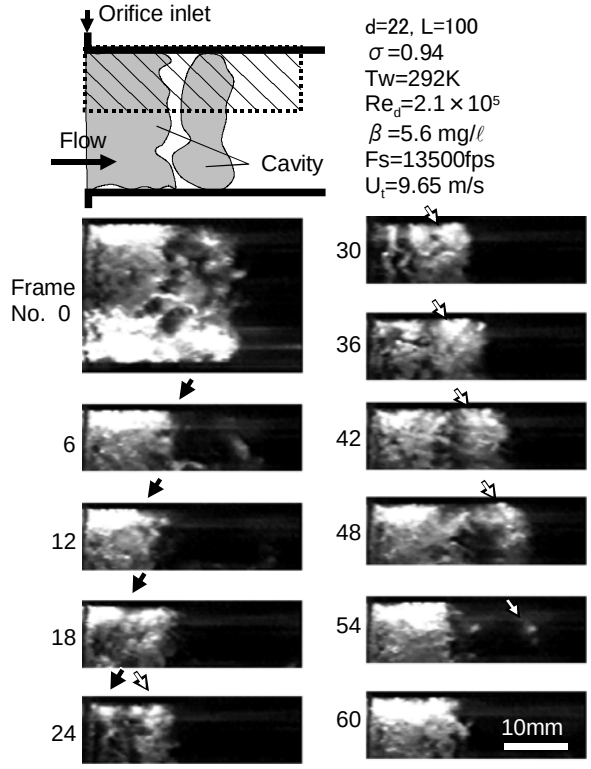

Fig.5 Behavior of cavity shedding and re-entrant motion [14]**.**

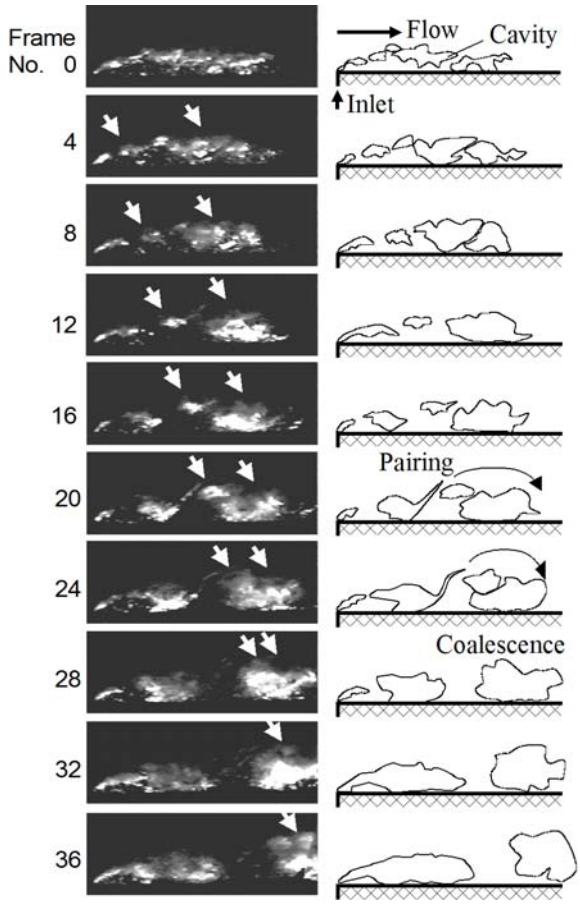

σ=0.94 , U_t=9.65 m/s , Re_d=2.1x10^5
β=3.0-3.5 mg/ℓ , Tw=294 K , Fs=18000fps

Fig.6 Behavior of cavity using laser sheet method at σ=0.94 [15]**.**

of $\sigma = 0.14$, it changes into the state of the jet flow being shed for a large-scale cavitation cloud. In addition, as pressure decreases, the downstream expansion creates a choking state, and the jet flow separates from the orifice inlet edge and floods downstream without reattachment to the orifice throat.

3.2. Unsteady Cavitation Behavior in the Orifice Throat

Unsteady shedding behavior of cavities is particularly observed when the cavity is limited to the inlet of the orifice at $\sigma = 0.93$. Cavity behavior on a separated shear layer is difficult to observe because cavities exist along the orifice wall in axi-symmetric flow fields in a circular cylindrical orifice. We visualize the cavity in the orifice throat by means of a metal halide light and a laser sheet. Here, the orifice is 22 mm in diameter, 100 mm in length, and has no inlet roundness.

Figure 5 shows the result of observation around the inlet of the orifice [14], where only the upper and lower parts of the cavity can be illuminated. In this case, we show the behavior of the upper cavity (the images after Frame 6 show only the upper half of the image of Frame 0). A re-entrant motion [1],[11],[16] appears at the trailing edge of an attached cavity around Frame 6 (black arrows in Fig. 5). Then the re-entrant motion moves upstream (Frames 6 – 24) and reaches the leading edge of the attached cavity around Frame 24. This re-entrant motion appears uniformly around the circumference of the orifice wall. The mean velocity of the re-

entrant motion, *Ur,* can be estimated as about *Ur* = 11 m/s that almost equals the mean velocity at the orifice throat (*Ut* = 9.6 m/s).

In Frame 24, after the re-entrant motion reaches the leading edge, some small vortex cavities appear on the separated shear layer. These vortex cavities move downstream with coalescence and growth motion. It is worth noticing that the re-entrant motion, coalescence and growth motion, and periodic shedding of the cavities appear with the self-induced vibrations.

We performed more detailed observation using a laser sheet [15]. Figure 6 shows a characteristic example at σ = 0.94, in the transition cavitation stage, in which cavities grow to a large scale and shed periodically. Only lower cavities are shown because the cavity is illuminated by the laser sheet from the lower direction of the test section. Some small vortex cavities on the separated shear layer form a large-scale cavitation cloud with pairing and coalescence motion. Here, the mean moving velocity of the shedding cavity, *Uv*, can be estimated at about *Uv* = 10 m/s. The flow velocity, *Uc*, at a contraction part of the orifice entrance is evaluated as *Uc* = 16m/s under the coefficient of contraction of 0.62. The ratio of the passing speed of the vortex cavity to the velocity of the main stream at the contraction part, *Uv/Uc*, is evaluated at about 0.6. This value corresponds to the result for the passing speed of the vortex on the shear layer around a thick plate shown by Kiya [18].

3.3. Behavior of Large-scale Cavitations downstream of the Orifice

A large-scale cavitation cloud is formed downstream of the orifice with a further decrease in the cavitation number, as shown in Fig. 7. Here, the orifice has *L*=70 mm long and *d*=15 mm in diameter with inlet roundness of *R*=10 mm in radius. A large-scale cavity is shed downstream periodically with a relatively low frequency. A re-entrant motion that rushes upstream is observed around Frames from -1000 to -800 in Fig. 7. The motion reaches the leading edge of the cavity around Frame -800 (Collapse I). At that time, the cavity is broken and shed downstream. Then the shedding cavity collapses around Frame -600 (collapse II). This behavior appears periodically (re-entrant motion: Frames from -300 to -200; shedding motion: Frames from -150 to 0). In such cases, the flow field in a typical single-phase state is greatly disturbed and forms the particular flow state of the cavitating flow.

Figure 7(b) shows a result of the image analysis using the frame difference method. Some black and white bands can be observed. The black region in the figure indicates small bubble collapse and the white region corresponds to growth and movement of the cavitation cloud. Some white bands corresponding to movement (growth) of cavity are shown straight. It is shown that the cavity moves (grows) at a constant speed of about 2 m/s from the image analysis. Some black regions indicate small bubbles collapse. The regions around *x* = 0-50 mm at Frames -850 and 280, and *x* = 250-350 mm at Frames -600 and 0 correspond to collapse I and collapse II, respectively. These black bands are approximately in parallel with a horizontal axis. That is, it is a high speed phenomenon.

In addition, Fig. 8 shows an interesting behavior related to pressure wave propagation caused by the cavity collapse around Frame 0 in Fig.7. A bright region, related to a small bubble collapse, propagates radially around the Frames 1–7, as shown in Fig. 8(a). This behavior corresponds to the propagation of a pressure wave caused by cavity collapse. Still images do not provide a clear view of the behavior, although the propagation of small bubble collapse can be observed clearly in a movie. Thus, we made an estimation using image analysis. Figure

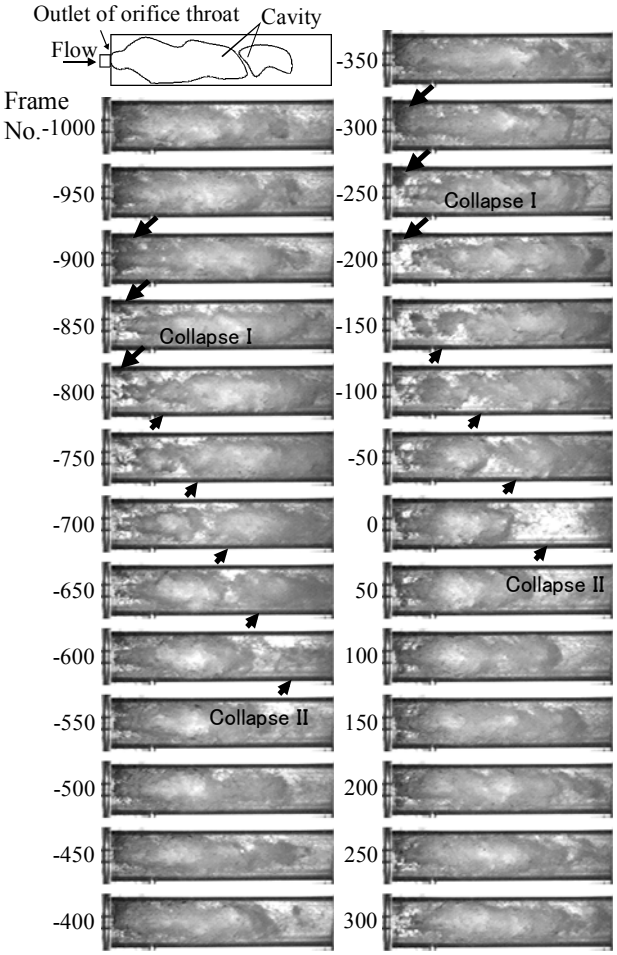

(a) Behavior of bubble collapse

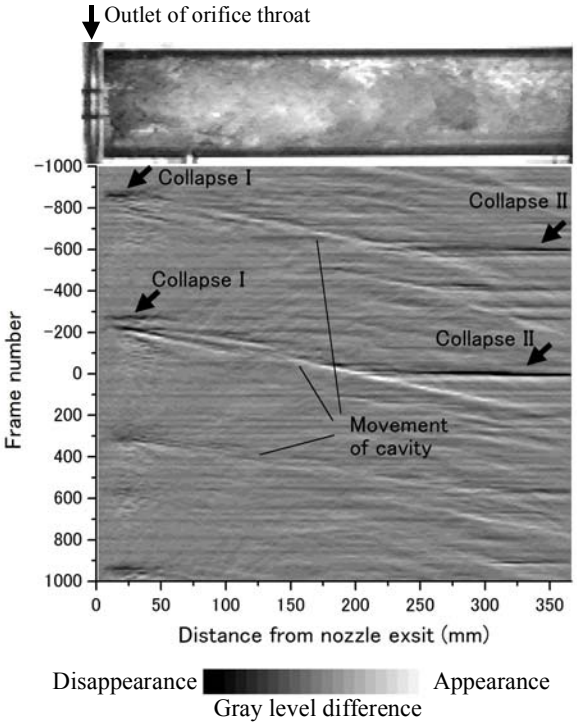

(b) Result of image analysis

σ=0.097, U_t=13.2 m/s, Re_d=2.88x10^5, β=1.35 mg/ℓ, Fs=9000 fps
L=100, d=22, R=10

Fig.7 Cavity behavior downstream of orifice.

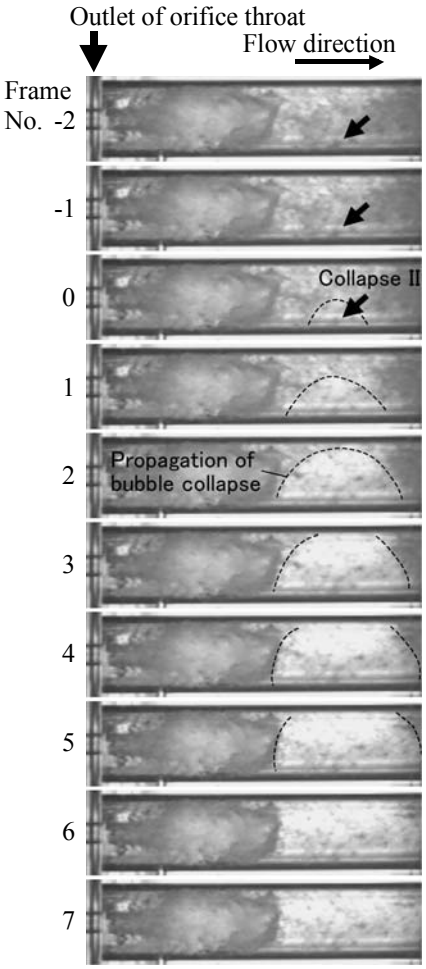

(a) Propagation of bubble collapse

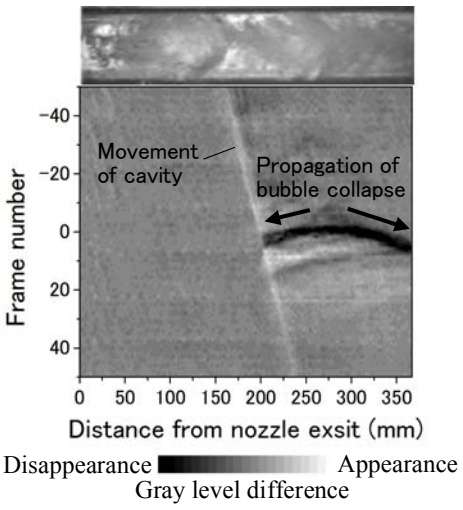

(b) Result of image analysis

σ=0.097, U_t=13.2 m/s, Re_d=2.88x10^5,
β=1.35 mg/ℓ, Fs=9000 fps

Fig.8 Propagation of bubble collapse downstream of orifice.

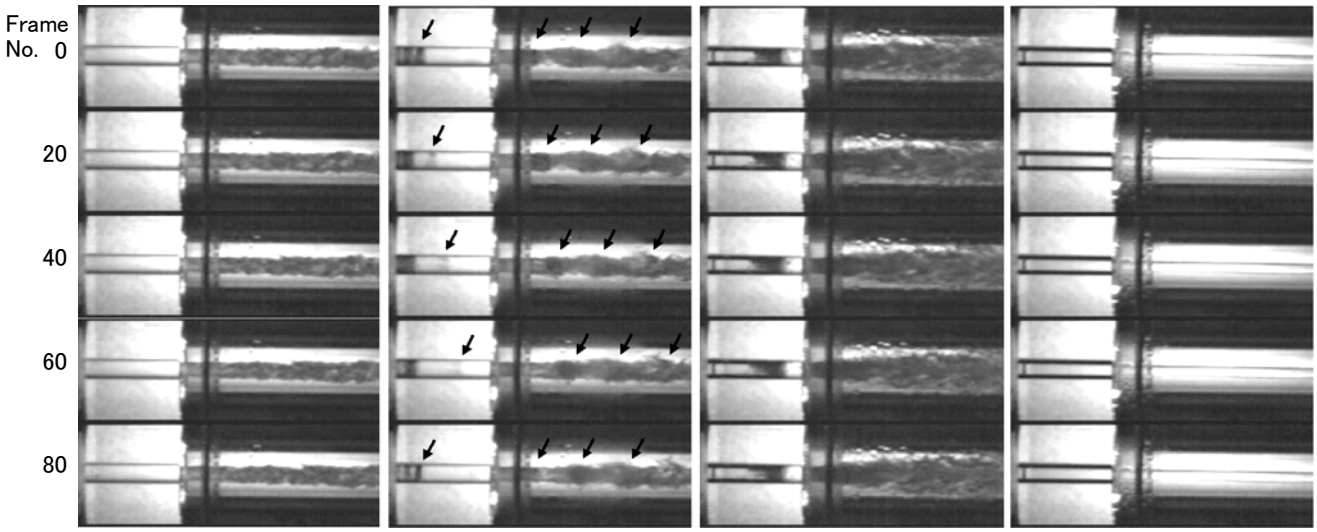

(a) σ=1.32 (b) σ=0.96 (c) σ=0.85 (d) σ=0.79

L=70, d=15, R=0: $Re_d=1.4\times10^5$, β = 2.0-3.9 mg/ℓ, Q=0.1m³/min

Fig.9 Behavors of liquid jet in air.

8(b) shows a result of the image analysis using the frame difference method. A black region corresponding to the cavity collapse appears around Frame 0. This black region propagates upstream and downstream with a lapse of time. This propagation speed of small bubble collapse was estimated to be approximately 100–150 m/s. Further examination of the decrease in speed of sound in the gas-liquid multi-phase state is needed.

3.4. Behavior of the Cavity in the Orifice Throat and Liquid Jet downstream of the Orifice

Let us consider a jet in air downstream of the orifice. The liquid jet flow is realized by filling the air in the test section downstream of the orifice after the cavitation in the orifice throat is set. Here, the orifice is L=70 mm long and d=15 mm in diameter without inlet roundness. Figure 9 shows the cavitation behavior in the orifice throat and liquid jet downstream of the orifice. The liquid jet separates at the exit of the orifice and gushes in a non-cavitating condition, as shown in Fig. 9(a). The surface of the liquid jet is relatively smooth and its periodicity is not observed. Figure 9(b) shows the behavior in a cavitation state corresponding to the transition cavitation stage that sheds cavitation periodically. In this case, the liquid jet surface is disturbed periodically (see arrows in the figure). This disturbance is related to the cavitation behavior in the orifice throat. This characteristic jet behavior will be discussed later. The cavitation increases until the latter half of the orifice throat and an irregular vibration and the shedding behavior are observed at the trailing edge of the cavity in Fig. 9(c). The flow separates at the inlet of the orifice throat and reattaches around the trailing edge of the cavity, it then separates at the exit of the orifice and gushes downstream. Here, the jet spreads radially due to a disturbance by the cavity. In the case of Fig. 9(d), the cavitation changes to a supercavitation state. The flow separates at the orifice throat inlet and gushes downstream without re-attachment in the orifice throat. The liquid jet surface is smooth.

3.5. Unsteady Behavior of the Liquid Jet and Cavitation in the Orifice Throat

It is understood that the jet flow gushing from the orifice, as mentioned above, is greatly influenced by the cavitation behavior in the orifice throat. In Fig. 9 (b), the effect becomes remarkably visible. Figure 10 shows the result of measuring the time change at the disturbed

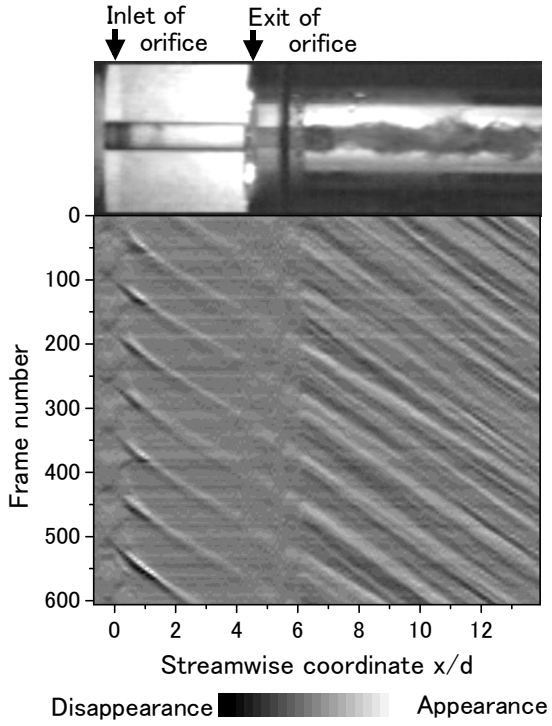

L=70, d=15, R=0: σ=0.96, Re_d=1.0 × 10^5
β = 2.0-3.9 mg/ℓ, Q=0.06-0.11m^3/min

Fig.10 Result in image analysis of behaviors of liquid jet and unsteady cavitation.

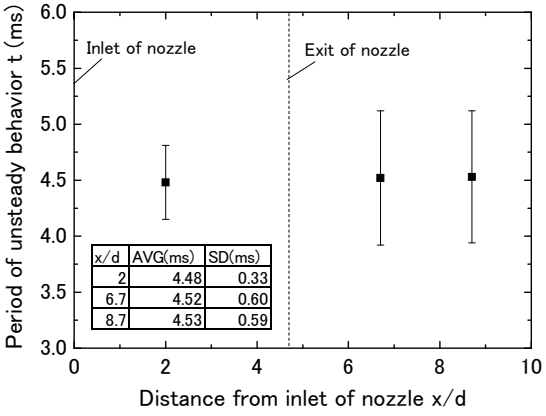

x/d	AVG(ms)	SD(ms)
2	4.48	0.33
6.7	4.52	0.60
8.7	4.53	0.59

L=70, d=15, R=0: σ=0.96, Re_d=1.0 × 10^5
β = 2.0-3.9 mg/ℓ, Q=0.06-0.11m^3/min

Fig.11 Period of unsteady liquid jet and cavitation in the nozzle.

position of the jet surface and the cavitation in the orifice throat, by image analysis, where the region of $x/d < 4.7$ corresponds to the orifice throat and $x/d > 4.7$ corresponds to a region of liquid jet. The area where the white region is parallel to the black indicates cavity movement. Shedding of cavitation in the orifice throat and disturbance of the liquid jet surface appear periodically and move linearly (with a constant velocity). Moreover, disturbances in the liquid jet appear in the extension of the movement of the cavitation in the orifice throat. Figure 11 shows a change in periods of cavity shedding in the orifice throat (in the region of $x/d < 4.7$) and disturbance of the liquid jet (in the region of $x/d > 4.7$). A Strouhal number St is defined as $St = d/TU$ (T: a period of cavity shedding in the orifice throat or disturbance of the liquid jet) and its value is about 0.3–0.5 in both regions. The movement velocity of shedding cavities and disturbance parts of the liquid jet were estimated at about 7–10 m/s, the same as the flow velocity at the orifice throat, suggesting that flow disturbances caused by cavities in the orifice throat are convected by the flow and are connected with disturbances of the liquid jet surface.

As mentioned above, the behavior of the liquid jet surface was affected to a considerable degree by the cavitation state in the orifice throat and the separation state.

4. CONCLUSIONS

Unsteady phenomena related to cavitation were investigated through high-speed visualizations in a flow field downstream of a circular cylindrical orifice.

(1) Jet behaviors in a orifice and downstream of the orifice were observed by examining a liquid jet in both air and liquid with a closed-loop cavitation tunnel.
(2) Unsteady behavior of cavitation cloud appears even if the upstream flow condition is steady state.

(3) Pressure wave effects, caused by the collapse of the cavitation cloud, can be estimated through high-speed observations and the image analysis.
(4) Disturbances due to the collapse of cavities within the orifice throat are convected downstream and related to the instability of the liquid jet surface.

REFERENCES

1. R. T. Knapp, *Cavitation*, McGraw-Hill (1970).
2. A. Yamaguchi and S. Shimizu, "Erosion Due to Impingement of Cavitating Jet", *Trans. ASME, J Fluid Eng,* **Vol. 109**, pp.442-447 (1987).
3. H. Soyama et al., "High-Speed Observation of the Cavitation Cloud around a High-Speed Submerged Water Jet", *JSME Int. J., Ser B*, **Vol.38**, **No.2**, pp. 245-251 (1995).
4. A. Sou et al., "Effects of Cavitation in a Nozzle on Liquid Jet Atomization", *JSME Int. J., Ser B*, **Vol.49**, **No.4**, pp. 1253-1259 (2007).
5. K. Sato, "A Study of Cavitation Process by means of Acoustic Pulse Measurement", *Proceeding of ASME FED-57*, pp. 115-121 (1987).
6. K. Sato and N. Ogawa, "Collapsing Behavior of Vortex Cavitation Bubbles in the Wake of a Circular Cylinder", *Proceeding of ASME FED-226*, pp. 119-125 (1995).
7. K. Sato and S. Kondo, "Collapsing Behavior of a Vortex Cavitation Bubble near Solid Wall: Spanwise-view Study", *Proceeding of ASME FED-236*, pp. 485-490 (1997).
8. K. Sato et al., "Observations of Chain-Reaction Behavior at Bubble Collapse Using Ultra High Speed Video Camera", *Proceeding of ASME FEDSM'03*, FEDSM2003-45002 (2003).
9. K. Sato et al., "Bubble Collapsing Behavior and Damage Pits of Separated Vortex Cavitation", *Proceeding of 3rd Int. Symp. on Cavitation*, Grenoble, **Vol. 2**, pp. 157-162 (1998).
10. K. Sato and Y. Saito, "Cavitation Bubble Collapse and Impact in the Wake of a Circular Cylinder", *Proceeding of 5th Int. Symp. on Cavitation*, Osaka, Cav03-GS-11-004 (2003).
11. K. Sato et al., "Observations of Unsteady Separeated-type Cavitation in Convergent-Divergent Channel", *Proceeding of 3rd Int. Symp. on Measurement Techniques for Multiphase Flow*, Fukui, pp. 203-210 (2001).
12. K. Sato and S. Shimojo, "Detailed Observations on a Starting Mechanism for Shedding of Cavitation Cloud" *Proceeding of 5th Int. Symp. on Cavitation*, Osaka, CAV03-GS-4-009 (2003).
13. K. Sato, Y. Saito, and H. Ota, "Impulsive Behavior of Cavitation Bubbles in a Circular-Cylindrical Orifice Flow", *Proceeding of ASME FEDSM2000,* Cavitation and Multi-Phase Flow Forum, FEDSM2000-11023, (2000).
14. K. Sato, and Y. Saito, "Unstable Cavitation Behavior in a Circular-Cylindrical Orifice Flow", *JSME Int. J. Ser. B*, **Vol. 45**, **No. 3**, pp. 638-645 (2003).
15. Y. Saito, and K. Sato, "Growth Process to Cloud-like Cavitation on Separated Shear Layer", *Proceeding of ASME FEDSM2003,* Cavitation and Multi-Phase Flow Forum, FEDSM2003-45007, (2003).
16. Y. Saito and K. Sato, "Bubble Collapse Propagation and Pressure Wave at Periodic Cloud Cavitation", *Proceeding of 6th Int. Conf. on Multiphase Flow*, Leipzig, Germany, Paper No. S7_Tue_C_24 (2007).
17. Y. Sugimoto and K. Sato, "Visualization of Pressure Wave Generated By collapse of Cavitation cloud using Frame Difference Method," *Proceeding of 13th Int. Symp. Flow Visualization,* Nice, France, Paper 284 (2008).
18. M. Kiya and K. Sasaki, "Structure of a Turbulent Separation Bubble", *J. Fluid Mech.*, **Vol.137**, pp. 83-113 (1983).